Sorted and Aligned Single-Walled Carbon Nanotube Networks for Transistor-Based Aqueous Chemical Sensors

Mark E. Roberts, Melburne C. LeMieux, and Zhenan Bao*

Department of Chemical Engineering, Stanford University, Stauffer III, 381 North-South Mall, Stanford, California 94305-5025

ABSTRACT Detecting trace amounts of analytes in aqueous systems is important for health diagnostics, environmental monitoring, and national security applications. Single-walled carbon nanotubes (SWNTs) are ideal components for both the sensor material and active signal transduction layer because of their excellent electronic properties and high aspect ratio consisting of entirely surface atoms. Submonolayer arrays, or networks of SWNTs (SWNTnts) are advantageous, and we show that topology characteristics of the SWNT network, such as alignment, degree of bundling, and chirality enrichment strongly affect the sensor performance. To enable this, thin-film transistor (TFT) sensors with SWNTnts were deposited using a one-step, low-cost, solution- based method on a polymer dielectric, allowing us to achieve stable low-voltage operation under aqueous conditions. These SWNT-TFTs were used to detect trace concentrations, down to 2 ppb, of dimethyl methylphosphonate (DMMP) and trinitrotoluene (TNT) in aqueous solutions. Along with reliable cycling underwater, the TFT sensors fabricated with aligned, sorted nanotube networks (enriched with semiconductor SWNTs) showed a higher sensitivity to analytes than those fabricated with random, unsorted networks with predominantly metallic charge transport.

KEYWORDS: carbon nanotube sensor · aqueous electronic sensor · low-voltage transistor · plastic electronics · SWNT transistor

Electronic materials with inherent nanoscale features are ideal components for next-generation autonomous sensor technology by efficiently combining excellent detection sensitivity with ballistic charge transport (transduction) in a single layer of material. Such electronic sensors based on nanomaterials are well suited for a variety of applications from lab-on-chip and *in vivo* biosensors to environmental monitoring and national defense. They offer a high ratio of detection sensitivity to cost, can potentially operate remotely with low power demands, and their material composition affords low-profile or transparent systems. Electronic signal transduction of chemical/biological environmental analytes is advantageous over conventional optical methods, owing to lower cost and less device complexity, increased sampling rates, and improved portability. We can therefore envision a flexible, robust sensor platform that relies on electronic signal transduction with low-voltage, allowing for reliable and stable operation in ambient and aqueous environments over a reasonable time period. SWNTs exhibit superior electronic and mechanical properties, in addition to environmental stability, yielding ideal components for flexible electronic devices.[1,2]

SWNTs are particularly interesting as the active material for biological and chemical sensors. Their unique geometry consisting of a one-dimensional electronic material comprising only surface atoms means charge transport can be directly influenced by molecular absorbates.[3−5] While thin-film transistors (TFTs) based on SWNTs constitute an optimal platform for the molecular level detection of an array of analyte types, several obstacles still inhibit practical implementation. Individual SWNT-based devices are not feasible for large scale integration at this time; however, recently developed random nanotube networks[6,7] offer an excellent compromise with on/off ratios up to 10^5 after optimization of tube chirality ratio and/or device geometry.[8,9] Still, the nature of SWNTnt randomness in terms of chirality, tube density, and bundling makes device reproducibility poor, greatly inhibiting SWNT sensors and the understanding of how these elements affect analyte sensitivity and response.

Multiple types of SWNT devices have been demonstrated for analyte detection,[10] including chemiresistors,[11] chemicapacitors,[12] and chemFETs.[5] SWNT chemiresistor sensors operate by a change in conductance due to a relatively stronger charge transfer interaction, as opposed to weaker dipole or van der Waals interactions. Thus, they respond to a limited range of analytes,

*Address correspondence to zbao@stanford.edu.

Received for review July 15, 2009 and accepted September 11, 2009.

Published online September 21, 2009.
10.1021/nn900808b CCC: $40.75

but demonstrate good sensitivity to primarily aromatic molecules through effective $\pi-\pi$ stacking. SWNT chemicapacitors offer higher sensitivity to polarizable adsorbates, which respond to the high electric field surrounding the SWNTs generated from the applied bias.[12] This approach is limited to molecules with strong dipole moments and suffers from relatively slow response times.[12] More importantly, with regards to fluidic environments, the high dielectric constant of water would result in screening of the electric field around the SWNTs making this method ineffective for detection in aqueous media,[13] necessary for the applications previously described.

SWNT chemFET sensors have many distinct advantages over chemiresistors, including the ability to amplify the detection signal with the additional (gate) electrode. For sensor applications, an increased difference between "on" and "off" currents (on/off ratio) will produce a larger electronic response, and thus provide a larger signal for analyte detection. This requires that the SWNT networks consist of predominantly semiconducting nanotubes (scSWNTs).[15] TFTs based on scSWNTs respond to a wider range of analyte interactions than metallic SWNTs (metSWNTs) because of a reduced density of states near the Fermi level in metallic tubes as compared with the valence band edge of scSWNTs.[2,14,15] However, depositing a network of semiconducting scSWNTs from solution is nontrivial, and the electrical properties of the mixed films are generally dominated by the presence of metSWNTs.

Controlling the alignment and density of the SWNTs is another critical issue facing SWNT-based sensors, as recent studies have shown that the density of SWNTs strongly affects sensor performance.[16] While several groups have shown that nanotube networks can be fabricated,[17,18] other than a few,[6] most reports indicated the lack of control in terms of alignment, density, and bundling. Random aligned networks composed of bundles and multilayer SWNTs films often result in low on/off ratios due to metallic pathways dominating charge transport. This morphology can also suffer from a slow, ambiguous sensor response owing to the gradient in analyte concentration felt by 'buried' nanotubes. Therefore, the preferred SWNT chemFET sensors should have high on/off ratios and consist of a monolayer or submonolayer of primarily scSWNTs. The moderate to low surface density of nanotubes with enrichment of semiconducting SWNTs can potentially result in enhanced interactions compared to unsorted nanotubes since the analyte-SWNT binding energy depends on chirality.[19] These issues not only prevent random SWNT networks from acting as reproducible sensor elements, but inhibit a fundamental understanding of their response mechanisms. We resolve this issue using a deposition method that can enrich scSWNTs and align them in a one-step solution deposition process by controlling substrate surface chemistry on silicon[20] and polymeric films.[21] This self-sorting method results in a submonolayer of moderately aligned SWNTs enriched with semiconducting, unbundled nanotubes of reproducible density and alignment from device to device.

Previously, we demonstrated high performance TFTs with scSWNT networks on a chemically modified polymer gate dielectric layer with operating biases below 1 V.[21] Our solution deposition method is compatible with polymeric dielectric layers enabling integration with flexible substrates. Here, we demonstrate highly sensitive chemical sensors using these devices, with the detection of benchmark threats including dimethyl methylphosphonate (DMMP) and trinitrotoluene (TNT) down to 2 parts per billion (ppb) in aqueous solutions. Importantly, we show that the degree of alignment, bundling, and the chirality of the nanotube network play crucial roles in the sensor characteristics. We observed a markedly different sensor response for partially aligned SWNT networks enriched with semiconducting tubes (sorted networks) as opposed to unsorted, randomly oriented networks with a higher degree of bundled tubes. These results indicate that a careful control of the SWNT active network leads to improved sensor characteristics, while perhaps providing a platform to observe and understand SWNT/molecule interactions. Our ultimate goal is to demonstrate that the design approach discussed here for a highly stable nanotube electronic material may be promising for reliable, low-profile sensors.

RESULTS AND DISCUSSIONS

The fabrication of SWNT-based TFTs has been reported elsewhere.[21] Briefly, polymer dielectrics consisting of poly(4-vinylphenol) cross-linked with 4,4′-(hexafluoroisopropylidene)-diphthalic anhydride (HDA)[22] were deposited *via* spin coating to a thickness of 25 nm with a capacitance of 165 nF/cm^2. The PVP surface was subsequently modified with amine functionality using aminopropyltriethoxysilane (APTES) in a solution of anhydrous toluene. Sorted (semiconducting) and unsorted (metallic) SWNT networks were then deposited on the APTES-modified PVP substrates *via* spin-coating as described in the materials and methods section. Atomic force microscopy (AFM) images at two different magnifications shown in Figure 1 highlight the contrast between the sorted and unsorted networks and their topologies. Figure 1 panels B and C show the unsorted networks over small and large scales, respectively. At small scales, large (50−100 nm) bundles are observed while at larger scales, the poor uniformity in alignment and density is obvious. On the other hand, Figure 1 panels D and E show that the sorted SWNTnts possess well ordered, highly aligned debundled tubes at small and large scales, respectively. These sorted SWNTnts are enriched with scSWNTs as confirmed by mapping μ-Raman spectroscopy and

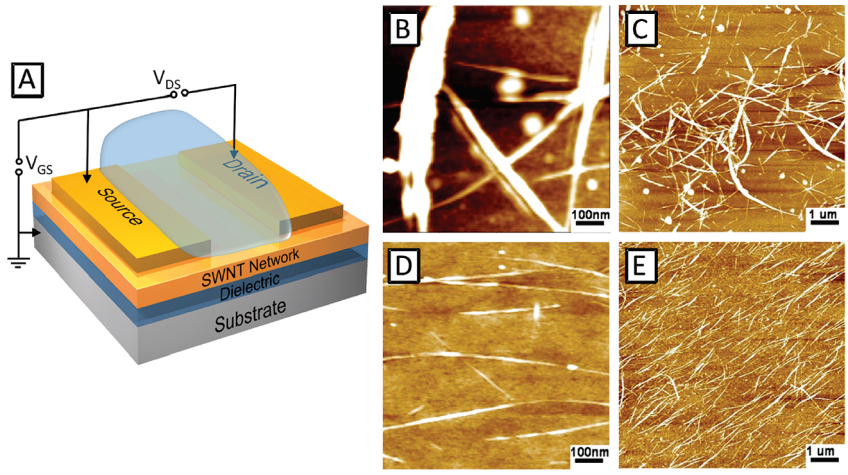

Figure 1. SWNT-TFT sensor schematic and SWNT network topology. (A) Illustrative schematic of a TFT with a SWNT network under aqueous conditions. (B) AFM topography images of an unsorted SWNT networks at high and (C) low resolution, *z*-scale is 50 nm. (D) AFM images of a sorted SWNT network at high and (E) low resolution, *z*-scale is 10 nm.

electrical characteristics discussed in a previous report.[21]

Top-contact thin-film transistors ($L = 50$ μm, $W = 1$ mm) were completed by thermally evaporating gold electrodes on top of the SWNT networks. Typically, devices fabricated using this method had an effective mobility (μ_{eff}) ranging between 1 and 6 $cm^2/(V\ s)$ with the highest at 13.4 $cm^2/(V\ s)$ and an average on/off ratio of 1.6×10^3 at a bias of -1 V. The effective mobility was determined using the geometry of the top-contact gold electrodes rather than correcting for the actual number of nanotubes spanning the channel. SWNT-based TFTs were also fabricated on plastic substrates with an ITO gate electrode; however, the electrical characteristics were slightly diminished ($\mu_{eff} \approx 0.7$ $cm^2/(V\ s)$) because of the rougher surface.

It is well-known that SWNTs function effectively as vapor sensors.[23] To demonstrate the potential for durable chemical sensors in aqueous environment, the SWNT TFTs were electrically characterized in water. No additional treatment or encapsulation was applied to the TFT substrates before immersion in water. The source-drain and gate biases (V_{DS}, V_{GS}) were limited to -0.6 V to keep the parallel ionic current through the solution minimal.[24] Before exposure to water, the TFT characteristics were calculated for $V_{DS} = V_{GS} = -0.6$ V, yielding typical effective charge carrier mobility ($\mu_{eff,}$), threshold voltage (V_T), and on/off ratio values of 1.2 $cm^2/(V\ s)$, 0.24 V, and 1.1×10^3, respectively. The μ_{eff} was determined using the geometry of the source-drain electrodes and no modifications were made to account for the *W/L* of the actual percolated network. The characterization in water leads to a general reduction in device performance yielding μ_{eff}, V_T, and on/off ratio values of 0.52 $cm^2/(V\ s)$, 0.38 V, and 10^2, respectively. In TFTs consisting of an organic semiconductor film (*e.g.*, 5,5′-bis-(7-dodecyl-9H-fluoren-2-yl)-2,2′′-bithiophene (DDFTTF)), we previously observed a gradual shift in performance with time as water diffused toward the semiconductor−dielectric interface;[22] however, when using submonolayers of SWNTs as the active material, the shift in electrical characteristics occurs within 2 s of water exposure. The direct access of semiconducting SWNT network in immediate proximity of the dielectric surface to the bulk aqueous solution is ideal for highly sensitive sensors. The lower on/off ratio in water is a result of higher off-current arising from an increase in conductance across the electrodes, and the lower mobility is most likely due to charge scattering caused by water absorption[13,25] and doping of nanotubes.[13] Despite the slightly lower on/off ratio around 10^2, the SWNT TFTs were extremely stable in water, illustrating a stable drain current, I_{DS}, for over 400 electrical cycles of $V_{GS} = 0.6$ to -0.6 V with $V_{DS} = -0.6$ V, as shown in Figure 2. After removing the water and drying under a stream of nitrogen, the performance of the SWNT TFTs returned to the previous values measured in air, indicating there is no degradation of the SWNTs or the dielectric layer.

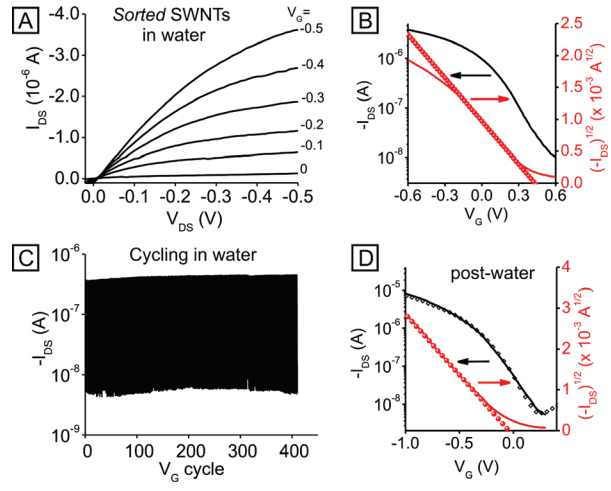

Figure 2. Transistor characteristics of TFTs with SWNT networks under aqueous conditions. (A) Output characteristics ($I_{DS}-V_{DS}$) measured in water for a TFT with a sorted SWNT network; (B) Transfer characteristics $I_{DS}-V_{DS}$ of the same device in panel A; (C) Repeated $I_{DS}-V_{DS}$ cycles (400 times) in water showing no device degradation; (D) Post-water-exposure transfer characteristics (dashed curves are the characteristics before exposure to water) showed no significant change compared to the initial characteristics (Panels A, B, and D were reprinted from ref 21. Copyright 2009, American Chemical Society).

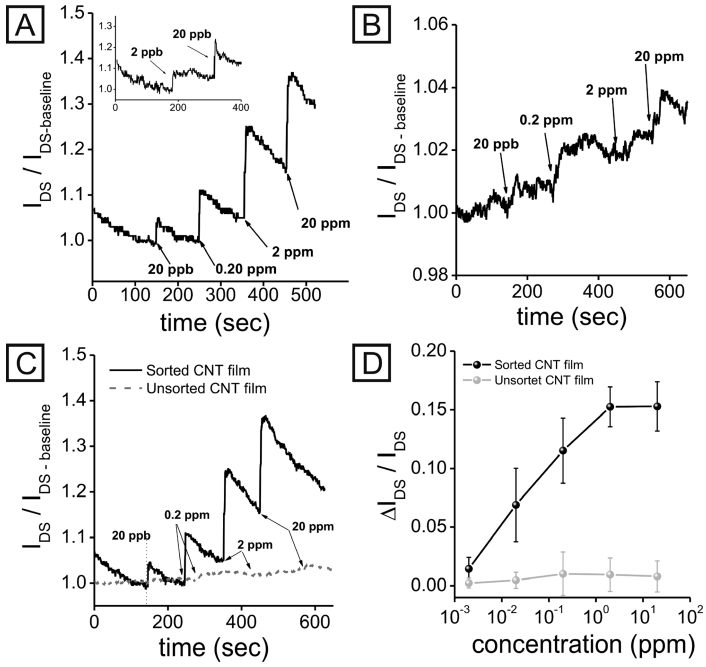

Figure 3. Sensor response to DMMP for sorted (sc) and unsorted (met) SWNT networks. (A) Normalized drain current (I_{DS}/I_{DS-0}), relative to the initial baseline, of TFTs with a sorted SWNT network upon exposure to dilute solutions of DMMP with increasing concentration. (Inset) I_{DS}/I_{DS-0} for DMMP solutions down to 2 ppb. (B) Similar plot in A for TFTs with an unsorted (metallic) SWNT network. (C) Composite plot of A and B showing the stark contrast in I_{DS}/I_{DS-0} for TFTs with sorted (black) and unsorted (gray) SWNT networks. (D) The average relative response ($\Delta I_{DS}/I_{DS}$) for DMMP solutions with sorted (black) and unsorted (gray) networks with standard deviations shown by error bars.

TFTs based on CNTs are well-suited for chemical detection of explosive and chemical warfare agents because of their interactions with nitro and phosphonate groups. The contamination of 2,4,6-trinitrotoluene (TNT) in water supplies is of a great concern because of toxicity and mutagenicity effects, and its concentration at manufacturing, processing, and disposal sites can be as high as 100 mg/L in water.[26] Dimethyl methylphosphonate (DMMP) is another target of interest owing to its molecular similarity to nerve-agents, such as Sarin. Electronic detection of trace concentrations of DMMP and TNT was carried out by adding a small volume (2 μL) of the analyte solution to a water reservoir (8 μL) on the TFT channel (see Figure 1A) while the device was under bias ($V_{DS} = V_{GS} = -0.6$ V) with successively increasing concentration. Drain current measurements were recorded at 0.5 s increments since we anticipated rapid analyte responses. In the absence of any analyte (*i.e.*, DI water), no change in current was observed upon solution addition (Supporting Information, Figure SI-1). The normalized TFT drain current (I_{DS}/I_{DS-0}, where I_{DS-0} is a current before the analyte addition) as a function of DMMP concentration is shown in Figure 3. The inset shows the change in current in response to a 2 parts per billion (ppb) solution, which was performed on the same device in a subsequent trial after regenerating the TFT (applying a $V_{GS} = +0.6$ V, $V_{DS} = -0.6$ V for 60 s in DI water) to determine the TFT sensitivity.

Interestingly, previous studies have shown that ppb detection of DMMP was not possible unless the SWNTs were functionalized.[27] This is also the first demonstration of ppb level detection of DMMP in water and the best sensitivity reported to date for SWNT sensors operating in a fluidic environment. Most importantly, the sensor response was extremely rapid, occurring within 2 s of the analyte exposure, owing to the use of a submonolayer of unbundled SWNTs. On the contrary, TFTs with thin organic semiconductor films tend to have much slower responses due to the time it takes for the analyte to diffuse to the semiconductor−dielectric interface where the majority of the current flows. After the initial increase in current following the analyte dose, the current gradually decreases to a value greater than the baseline. This behavior has previously been observed for organic semiconductor films in which the analyte has direct access to the dielectric surface, which could be attributed to a slow reorganization of analyte and water molecules at the dielectric interface.[28] In water with pH around 6.8−7.2, the amine surface ($pK_a \sim 10$) is slightly charged and therefore results in strong electrostatic interactions with the analyte molecules in solution, thus depleting DMMP from the water and SWNT surfaces.

The drain current response of TFTs with semiconducting (sorted) SWNTnts to DMMP was compared to those fabricated with metallic (random) nanotube networks. The absolute current was higher for the devices with random networks, owing to the presence of metallic nanotubes. To account for this, the I_{DS} response curves were normalized by dividing by the baseline current before the addition of the analyte (I_{DS-0}). Essentially no response to DMMP solutions was observed, signifying the importance of nanotube type/chirality on the TFT response, and highlighting the fact that SWNT sensors based on chemiresistors, although easier to fabricate, are limited here. This attribute could be responsible for the variability in response of random networks comprising varying mixtures of metallic and semiconducting nanotubes. The increase in I_{DS} upon DMMP exposure for a sorted SWNT network (Figure 3A) is consistent with a dipole interaction model rather than a charge transfer process, which has been previously suggested in literature to explain a decrease in conductance from the electron donating nature of DMMP.[27] However, the relatively polar DMMP has a strong dipole moment which is more likely to result in local induced-dipole electrostatic interactions rather than charge transfer reactions.[12] Additionally, the rapid response and reversibility of these devices indicate that charge transfer reactions do not occur. Electrostatic interactions lead to gate-field perturbations, which influence the carrier mobility and density in the semiconducting SWNTs in the TFT channel, therefore, only

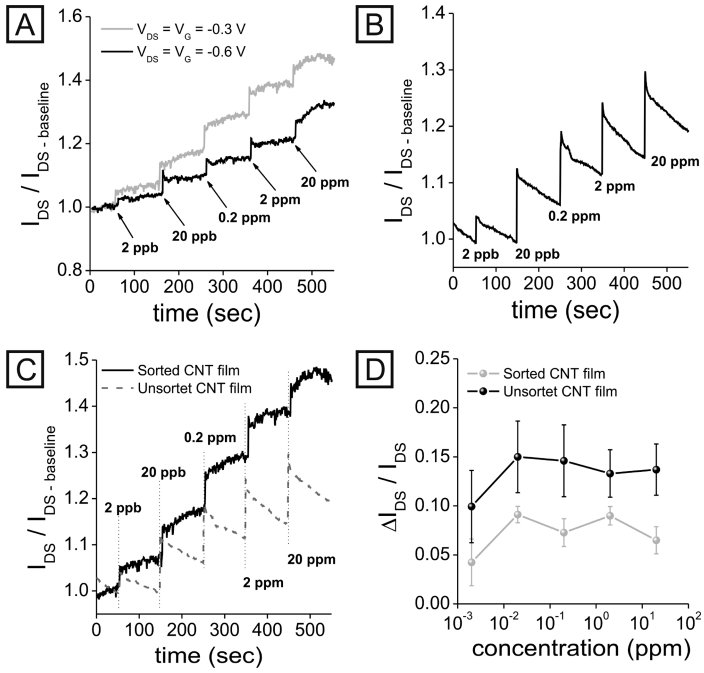

Figure 4. Sensor response to TNT for sorted (sc) and unsorted (met) SWNT networks. (A) I_{DS}/I_{DS-0} of a sorted SWNT network upon exposure to TNT solutions ranging from 2 ppb to 200 ppm for $V_{DS} = V_{GS} = -0.3$ V (gray) and $V_{DS} = V_{GS} = -0.6$ V (black). (B) I_{DS}/I_{DS-0} of an unsorted SWNT network upon exposure to TNT solutions ranging from 2 ppb to 200 ppm for $V_{DS} = V_{GS} = -0.3$ V. (C) Composite plot of A and B showing the I_{DS}/I_{DS-0} for TFTs with sorted (black) and unsorted (gray) SWNT networks. (D) The average relative response ($\Delta I_{DS}/I_{DS}$) for TNT solutions with sorted (black) and unsorted (gray) networks with standard deviations shown by error bars.

sorted SWNT networks are expected to show a significant response owing to their high on/off ratio. In the random SWNT networks, the current is dominated by the transport in the metallic tubes, which is only slightly modulated by gate voltage; therefore, little to no response to the DMMP analyte is expected. Indeed, devices with random nanotube networks—essentially chemiresistors—showed little to no response to DMMP solutions contrary to the TFTs with organized (semiconducting) nanotube networks.

The average TFT sensor response and standard deviation (from 3−4 devices with similar TFT performance) as a function of DMMP concentration is shown in Figure 3D for sorted and unsorted nanotube networks. The response ($\Delta I_{DS}/I_{DS}$) is calculated by normalizing the derivative of the I_{DS} *versus* time to I_{DS} before the analyte addition. A nearly linear response is observed for TFTs with sorted SWNT networks to DMMP solution concentrations ranging from 2 ppb to 2 ppm (Figure 3D), which saturates above 2 ppm, while almost no response is observed for the unsorted networks for any concentration.

Previously, Chen *et al*. reported that the junction between the nanotubes and metal contacts plays a key role in the SWNT-based sensor response to large protein molecules.[29] More recently, however, this mechanism was contested by Heller *et al*. in a report showing that the electrostatic gating of the bulk SWNTs was more significant than effects at the electrode junction.[30] While the nanotube-metal contact junction may play a role in the sensor response, most research groups find this effect to be negligible, especially for small molecule analytes.[25,27,31] The fact that we observe no response in a control experiment with pure water (Supporting Information, Figure SI-1) and highly contrasting responses from devices with different nanotube types to DMMP suggest that the response from nanotube-contact junction is not significant in our system.

Similar to DMMP, the SWNT TFTs were sensitive to trace concentrations of TNT in solutions of water and acetonitrile. Figure 4A shows the change in TFT current, normalized to the baseline (3.0×10^{-4} v/v acetonitrile/water), upon exposure to solutions of TNT with concentrations from 2 ppb to 20 ppm for $V_{DS} = V_{GS} = -0.3$ V and $V_{DS} = V_{GS} = -0.6$ V. A slight amount of acetonitrile was added to the water solution to match the volume of acetonitrile in the dilute TNT solutions. Again, the TFT response to the analyte solution was extremely rapid (less than 2 s). Interestingly, the relative sensor response to TNT solutions is enhanced when the TFT is biased at −0.3 V compared to −0.6 V, especially at lower concentrations (~2 ppb), which can be attributed to a steeper slope of the transfer characteristics ($I_{DS}-V_{GS}$) as shown in Figure 2B. In this region, the TFT current is more susceptible to local variations of the electrostatic environment, thus highlighting the advantage of using a 3-terminal TFT sensor compared to a 2-terminal chemiresistor to enhance the detection signal.

Contrary to their response to DMMP solutions, random (metallic) nanotube networks were also sensitive to TNT solutions (Figure 4B); however, the observed sensor response was independent of analyte concentration for both sorted and unsorted networks. Upon exposure to TNT, the change in TFT current arises from the $\pi-\pi$ interactions between the SWNT and the conjugated (aromatic) analytes, which are stronger for metSWNTs due to a larger polarizability compared to scSWNTs.[32,33] The I_{DS} gradually decreased toward the baseline following the initial current increase for similar reasons described above. Moreover, the adsorption of the charge-acceptor nitro group has been shown to be more favorable on metSWNTs than scSWNTs due to larger Fermi level charge density.[19,34] A recent *ab initio* model suggested that the $\pi-\pi$ interaction is most likely the dominant interaction between the SWNTs and TNT, albeit with a minor contribution from elec-

tron donation by the nitro group.[35,36] Since TNT is electron deficient, we expect an increase in the current upon charge transfer for both the sorted and unsorted network (p-type) TFTs.

On the basis of our proposed mechanisms, we can hypothesize that solutes with similar dipole moments or oxidizing power would elicit similar responses; however, we show that different nanotube types elicit unique responses. This is key step toward understanding the detection mechanism and moving toward the ultimate goal of chemospecificity. Furthermore, the results presented here demonstrate the importance of using a well-defined nanotube network/film for reproducible sensing applications. In future work, we will address specificity by incorporating different chiralities, functionalized surfaces, and specific receptor sites, among others.

CONCLUSION

The recent advances in SWNT processing leading to the ability to deposit carbon nanotubes in a self-sorting, aligned manner have triggered the potential for large scale manufacturing on rigid and flexible polymeric substrates. The incorporation of this self-sorting approach with polymer dielectrics *via* a room temperature, solution process represents a major step toward the realization of organized SWNT networks for flexible electronic applications, especially chemical detection. In this report, we have shown the good stability of our SWNT-based TFTs under water and the promise for aqueous chemical sensors with the detection of trace concentration of explosives and chemical warfare agents. Additionally, we highlighted the importance of network topology (*i.e.*, tube morphology and type) on the analyte response of SWNT-based TFT sensors, and demonstrated that a network of unbundled, primarily semiconducting nanotubes close to the percolation threshold provides good sensitivity and reversibility. We fabricated TFTs with either primarily semiconducting or metallic SWNT networks, which show starkly contrasting responses to TNT and DMMP solutions. The ability to assemble reproducible SWNT films and simultaneously control the deposited tube type provides a unique opportunity to investigate the fundamental properties of SWNT-based sensors. Our results provide insight into the mechanistic details for the interactions between carbon nanotubes and analytes with either weak dipole interactions or stronger charge transfer (*via* $\pi-\pi$ stacking). While more work is required to understand the full mechanistic details for all analyte types, the fact that we observe different responses with sorted and unsorted SWNTs emphasizes the importance of controlling the nanotube properties within the network.

MATERIALS AND METHODS

Thin-film transistors were fabricated and characterized as reported previously.[21] Briefly, sorted SWNT networks were deposited from a solution of 10 μg/mL of purified nanotubes in 1-methyl-2-pyrrolidone (NMP) (50 μL per cm^2 substrate) on an APTES-modified PVP substrate rotating at 3600−4000 rpm prior to solution addition. Unsorted SWNT networks were deposited in a similar manner on the APTES-modified PVP; however, the solution was allowed to settle on the surface for an extended period of time (60 s) before the substrate was spun dry. The samples were then dried in a vacuum oven (50 °C) for approximately 1.5 h to remove residual solvent, and stored under vacuum prior to the gold electrode deposition.

Electrical characterization in water was performed by placing a drop of deionized (DI) water (8 μL) across the source (S) and drain (D) electrodes such that the entire channel was covered; 20 μm diameter gold wires connected the S−D electrodes to the tungsten-tip probes. Immediately after the addition of water, the S−D current (I_{DS}) was measured *versus* gate voltage (V_{GS}) with a S−D bias that ranged from 0.6 to −0.6 V. Next, the output characteristics ($I_{DS}-V_{DS}$ for multiple V_{GS}) were measured. Sensor measurements were performed by measuring I_{DS} *versus* time with a constant V_{GS} and V_{DS}. V_{GS} was set to −0.6 V (−0.3 V) while the V_{DS} was set to −0.6 or −0.3 V, depending on the $I_{DS}-V_{GS}$ curves for the particular semiconductor SWNT film (noted in the results and discussion). Drain current measurements were recorded with 0.5 s increments. After a baseline was established (60−90 s), a drop of analyte solution (2 μL) was added to the droplet of water (8 μL). After the current stabilized, a solution with higher concentration was added to the existing droplet. This was repeated for multiple concentrations. The measurement continued until no change in I_{DS} was observed. After the measurement, a reverse bias (V_{GS} = 0.6 V) was applied for 60 s and the substrate was rinsed with water.

Acknowledgment. M.E.R. acknowledges partial support from the NASA GSRP fellowship. M.C.L. acknowledges support from the Intelligence Community Postdoctoral Fellowship Program. Z.B. acknowledges financial support from the Stanford Center for Polymeric Interfaces and Macromolecular Assemblies (NSF-Center MRSEC), NSF-EXP sensor program, and the Sloan Research Fellowship.

Supporting Information Available: Sensor control experimental data with DI water. This material is available free of charge *via* the Internet at http://pubs.acs.org.

REFERENCES AND NOTES

1. Baughman, R. H.; Zakhidov, A. A.; de Heer, W. A. Carbon Nanotubes—The Route Toward Applications. *Science* **2002**, *297*, 787–792.
2. O'Connell, M. *Carbon Nanotubes: Properties and Applications*; CRC Taylor & Francis: Boca Raton, FL, 2006; p 319.
3. Kong, J.; Dai, H. Full and Modulated Chemical Gating of Individual Carbon Nanotubes by Organic Amine Compounds. *J. Phys. Chem. B* **2001**, *105*, 2890–2893.
4. Allen, B. L.; Kichambare, P. D.; Star, A. Carbon Nanotube Field-Effect-Transistor-Based Biosensors. *Adv. Mater.* **2007**, *19*, 1439–1451.
5. Kauffman, D. R.; Star, A. Electronically Monitoring Biological Interactions with Carbon Nanotube Field-Effect Transistors. *Chem. Soc. Rev.* **2008**, *37*, 1197–1206.
6. Lay, M. D.; Novak, J. P.; Snow, E. S. Simple Route to Large-Scale Ordered Arrays of Liquid-Deposited Carbon Nanotubes. *Nano Lett.* **2004**, *4*, 603–606.
7. Artukovic, E.; Kaempgen, M.; Hecht, D. S.; Roth, S.; Gruner, G. Transparent and Flexible Carbon Nanotube Transistors. *Nano Lett.* **2005**, *5*, 757–760.

8. Collins, P. G.; Arnold, M. S.; Avouris, P. Engineering Carbon Nanotubes and Nanotube Circuits Using Electrical Breakdown. *Science* **2001**, *292*, 706–709.
9. Cao, Q.; Kim, H.-S.; Pimparkar, N.; Kulkarni, J. P.; Wang, C.; Shim, M.; Roy, K.; Alam, M. A.; Rogers, J. A. Medium-Scale Carbon Nanotube Thin-Film Integrated Circuits on Flexible Plastic Substrates. *Nature* **2008**, *454*, 495–500.
10. Snow, E. S.; Perkins, F. K.; Robinson, J. A. Chemical Vapor Detection Using Single-Walled Carbon Nanotubes. *Chem. Soc. Rev.* **2006**, *35*, 790–798.
11. Lay, M. D.; Novak, J. P.; Snow, E. S. Simple Route to Large-Scale Ordered Arrays of Liquid-Deposited Carbon Nanotubes. *Nano Lett.* **2004**, *4*, 603–606.
12. Snow, E. S.; Perkins, F. K.; Houser, E. J.; Badescu, S. C.; Reinecke, T. L. Chemical Detection with a Single-Walled Carbon Nanotube Capacitor. *Science* **2005**, *307*, 1942–1945.
13. Someya, T.; Kim, P.; Nuckolls, C. Conductance Measurement of Single-Walled Carbon Nanotubes in Aqueous Environment. *Appl. Phys. Lett.* **2003**, *82*, 2338–2340.
14. Gui, E.-L.; Li, L.-J.; Lee, P. S.; Lohani, A.; Mhaisalkar, S. G.; Cao, Q.; Kang, S. J.; Rogers, J. A.; Tansil, N. C.; Gao, Z. Electrical Detection of Hybridization and Threading Intercalation of Deoxyribonucleic Acid Using Carbon Nanotube Network Field-Effect Transistors. *Appl. Phys. Lett.* **2006**, *89*, 232104.
15. Lee, C. Y.; Strano, M. S. Understanding the Dynamics of Signal Transduction for Adsorption of Gases and Vapors on Carbon Nanotube Sensors. *Langmuir* **2005**, *21*, 5192–5196.
16. Wongwiriyapan, W.; Honda, S.; Konishi, H.; Mizuta, T.; Ohmori, T.; Kishimoto, Y.; Ito, T.; Maekawa, T.; Suzuki, K.; Ishikawa, H.; Murakami, T.; Kisoda, K.; Harima, H.; Oura, K.; Katayama, M. Influence of the Growth Morphology of Single-Walled Carbon Nanotubes on Gas Sensing Performance. *Nanotechnology* **2006**, *17*, 4424.
17. Rowell, M. W.; Topinka, M. A.; McGehee, M. D.; Prall, H.-J.; Dennler, G.; Sariciftci, N. S.; Hu, L.; Gruner, G. Organic Solar Cells with Carbon Nanotube Network Electrodes. *Appl. Phys. Lett.* **2006**, *88*, 233506.
18. Snow, E. S.; Novak, J. P.; Campbell, P. M.; Park, D. Random Networks of Carbon Nanotubes as an Electronic Material. *Appl. Phys. Lett.* **2003**, *82*, 2145.
19. Zhao, J.; Buldum, A.; Han, J.; Lu, J. P. Gas Molecule Adsorption in Carbon Nanotubes and Nanotube Bundles. *Nanotechnology* **2002**, *2*, 195.
20. LeMieux, M. C.; Roberts, M.; Barman, S.; Jin, Y. W.; Kim, J. M.; Bao, Z. Self-Sorted, Aligned Nanotube Networks for Thin-Film Transistors. *Science* **2008**, *321*, 101–104.
21. Roberts, M. E.; LeMieux, M. C.; Sokolov, A. N.; Bao, Z. Self-Sorted Nanotube Networks on Polymer Dielectrics for Low-Voltage Thin-Film Transistors. *Nano Lett.* **2009**, *9*, 2526–2531.
22. Roberts, M. E.; Mannsfeld, S. C. B.; Queralto, N.; Reese, C.; Locklin, J.; Knoll, W.; Bao, Z. Water-Stable Organic Transistors and Their Application in Chemical and Biological Sensors. *Proc. Natl. Acad. Sci. U.S.A.* **2008**, *105*, 12134.
23. Kauffman, Douglas R.; Star, A. Carbon Nanotube Gas and Vapor Sensors. *Angew. Chem., Intl. Ed.* **2008**, *47*, 6550–6570.
24. Fu, Q.; Liu, J. Effects of Ionic Surfactant Adsorption on Single-Walled Carbon Nanotube Thin Film Devices in Aqueous Solutions. *Langmuir* **2005**, *21*, 1162–1165.
25. Peng, G.; Tisch, U.; Haick, H. Detection of Nonpolar Molecules by Means of Carrier Scattering in Random Networks of Carbon Nanotubes: Toward Diagnosis of Diseases *via* Breath Samples. *Nano Lett.* **2009**, *9*, 1362–1368.
26. Talmage, S.; Opresko, D.; Maxwell, C.; Welsh, C.; Cretella, F.; Reno, P.; Daniel, F. Nitroaromatic Munition Compounds: Environmental Effects and Screening Values. *Rev. Environ. Contam. Toxicol.* **1999**, *161*, 1–156.
27. Lee, Chang Y.; Sharma, R.; Radadia, Adarsh D.; Masel, Richard I.; Strano, Michael S. On-Chip Micro-Gas-Chromatograph Enabled by a Noncovalently Functionalized Single-Walled Carbon Nanotube Sensor Array. *Angew. Chem., Intl. Ed.* **2008**, *47*, 5018–5021.
28. Roberts, M. E.; Mannsfeld, S. C. B.; Tang, M. L.; Bao, Z. Influence of Molecular Structure and Film Properties on the Water-Stability and Sensor Characteristics of Organic Transistors. *Chem. Mater.* **2008**, *20*, 7332–7338.
29. Chen, R. J.; Choi, H. C.; Bangsaruntip, S.; Yenilmez, E.; Tang, X.; Wang, Q.; Chang, Y.-L.; Dai, H. An Investigation of the Mechanisms of Electronic Sensing of Protein Adsorption on Carbon Nanotube Devices. *J. Am. Chem. Soc.* **2004**, *126*, 1563–1568.
30. Heller, I.; Janssens, A. M.; Mannik, J.; Minot, E. D.; Lemay, S. G.; Dekker, C. Identifying the Mechanism of Biosensing with Carbon Nanotube Transistors. *Nano Lett.* **2007**, *8*, 591–595.
31. Lee, C. Y.; Baik, S.; Zhang, J.; Masel, R. I.; Strano, M. S. Charge Transfer from Metallic Single-Walled Carbon Nanotube Sensor Arrays. *J. Phys. Chem. B* **2006**, *110*, 11055–11061.
32. Krupke, R.; Hennrich, F.; Lohneysen, H. v.; Kappes, M. M. Separation of Metallic from Semiconducting Single-Walled Carbon Nanotubes. *Science* **2003**, *301*, 344–347.
33. Lucas, L. A.; DeLongchamp, D. M.; Vogel, B. M.; Lin, E. K.; Fasolka, M. J.; Fischer, D. A.; McCulloch, I.; Heeney, M.; Jabbour, G. E. Combinatorial Screening of the Effect of Temperature on the Microstructure and Mobility of a High Performance Polythiophene Semiconductor. *Appl. Phys. Lett.* **2007**, *90*, 012112.
34. Seo, K.; Park, K. A.; Kim, C.; Han, S.; Kim, B.; Lee, Y. H. Chirality- and Diameter-Dependent Reactivity of NO_2 on Carbon Nanotube Walls. *J. Am. Chem. Soc.* **2005**, *127*, 15724–15729.
35. Woods, L. M.; Badescu, S. C.; Reinecke, T. L. Adsorption of Simple Benzene Derivatives on Carbon Nanotubes. *Phys. Rev. B* **2007**, *75*, 155415.
36. Star, A.; Han, T.-R.; Gabriel, J.-C. P.; Bradley, K.; Gruner, G. Interaction of Aromatic Compounds with Carbon Nanotubes: Correlation to the Hammett Parameter of the Substituent and Measured Carbon Nanotube FET Response. *Nano Lett.* **2003**, *3*, 1421–1423.